Phosphorus-31 Nuclear Magnetic Resonance of Ethidium Complexes with Ribonucleic Acid Model Systems and Phenylalanine-Accepting Transfer Ribonucleic Acid†

Evelyn M. Goldfield, Bruce A. Luxon, Vickie Bowie, and David G. Gorenstein*,‡

ABSTRACT: The temperature dependence of the ^{31}P NMR spectra of the ethidium complexes with poly(A)·oligo(U) and the ^{31}P spectra of phenylalanine tRNA (yeast) in various molar ratios of ethidium ion (Et) are presented. In the poly(A)·oligo(U)·Et complex, a new peak about 2.0 ppm downfield from the double-helix peak appears. We have assigned this peak to phosphates perturbed by ethidium. The chemical shift of this peak is consistent with the intercalation mode of binding and provides additional support for our hypothesis that ^{31}P shifts are sensitive probes of phosphate ester conformations. The main effect of ethidium on the ^{31}P spectra of $tRNA^{Phe}$ is the broadening of several of the scattered signals. These scattered signals are associated with phosphates involved in tertiary interactions. We propose that these broadened signals arise from phosphates near the Et binding site.

We have recently proposed that ^{31}P chemical shifts in phosphate esters may serve as a direct probe of P–O ester bond torsional angles. Both theoretical considerations [Gorenstein & Kar, 1975; see also Gorenstein (1975, 1978, 1981, 1983), Gorenstein & Goldfield (1982a,b), and Prado et al. (1979)] and direct experimental tests of this hypothesis [Gorenstein et al., 1976, 1982; Gorenstein & Luxon, 1979; see also Patel (1979a–d) and Gueron & Shulman (1975)] confirm that the ^{31}P signal of a phosphate diester monoanion in a gauche,gauche (*g,g*) conformation (as found in the helix state) should resonate several parts per million upfield from a diester in a nongauche conformation (as found in the random coil state).

These conclusions prove to be especially significant since other spectroscopic probes fail to provide detailed conformational information on the phosphate ester bonds in the nucleic acids. It is now believed that of the six torsional angles that largely define the conformational structure of the nucleic acids, the two P–O ester torsional angles provide the main conformational flexibility to the nucleic acid backbone (Kim et al., 1973; Sundaralingam, 1969). Thus, we have shown (Gorenstein et al., 1976, 1982) that ^{31}P nuclear magnetic resonance (NMR)[1] spectroscopy can monitor the "helix–coil" transitions in single-stranded nucleic acids. A large (0.7–1.3 ppm) downfield shift for a wide structural range of nucleic acids was observed when the temperature was raised. At low temperature, the nucleic acids will exist largely in a base-stacked, helical conformation with the phosphate ester predominantly in the gauche,gauche (*g,g*) conformation, while at higher temperatures, the nucleic acids will largely exist in random coil, unstacked conformations with the phosphate ester in an increased proportion of nongauche [i.e., gauche,trans (*g,t*) etc.] conformations [see, for example, reviews such as that of Ts'o (1975)].

In our previous studies (Gorenstein et al., 1982; Gorenstein, 1978, 1981), we have looked at the ^{31}P spectra of the model system poly(A)·oligo(U) in which separate ^{31}P signals are observed for the multistranded poly(A)·oligo(U) helix and the single-stranded forms of poly(A) and oligo(U). ^{31}P NMR was shown to provide a useful tool for direct estimation of the fraction of the different strand forms in solution. ^{31}P NMR spectroscopy has also proven useful in providing structural and dynamic information on transfer ribonucleic acid (tRNA) (Gueron & Shulman, 1975; Salemink et al., 1979, 1981; Gorenstein & Luxon, 1979; Gorenstein et al., 1981; Gorenstein & Goldfield, 1982a,b; Gorenstein, 1981, 1983).

In this paper, we examine the binding of ethidium to poly(A)·oligo(U) and to $tRNA^{Phe}$. ^{31}P NMR provides a convenient monitor of the phosphate ester conformational change occurring upon binding of drugs to nucleic acids.

^{31}P chemical shifts can potentially be used to determine the type of binding to the nucleic acids, e.g., intercalation vs. electrostatic binding. ^{31}P NMR can also be used to determine the degree of stabilization of the double helix in the nucleic acid systems by the drug.

The effect of Et on the ^{31}P NMR spectrum of tRNA will also prove useful in helping us to assign the individual ^{31}P signals to specific phosphates in the structure.

Experimental Procedures

NMR Spectra. All of the nucleic acids were obtained from either Sigma, P-L Biochemicals, Boehringer Mannheim, or Collaborative Research. The poly(A) and oligo(U) have an average length of 400 bases (P-L Biochemicals) and 20 bases (P-L Biochemicals), respectively. To safeguard against possible contamination of the biochemicals by paramagnetic metal ion impurities, we dissolved all biochemicals (except the tRNA) in double-distilled water and passed them through a column of Chelex-100 ion-exchange resin (Na^+ form) purchased from Bio-Rad Laboratories. The eluent was lyophilized, and the solid was dissolved in buffer solution for poly(A)·oligo(U) if it was to be used immediately or stored at −5 °C if it was to be used at some later time. The pH of the buffer–nucleic acid solutions was adjusted on a Radiometer Model PHM 64 research meter to a pH of 7.0. The tRNA samples were prepared as previously described (Gorenstein & Luxon, 1979). ^{31}P NMR spectra were recorded on a Bruker

† From the Department of Chemistry, University of Illinois, Chicago, Illinois 60680. *Received January 3, 1983.* Supported by research grants from the National Institutes of Health and the National Science Foundation. Purchase of the Bruker WP-80 spectrometer was assisted by a National Science Foundation Departmental Equipment Grant. Support of the Purdue Biological NMR facility by the National Institutes of Health (Grant RRO 1077) is acknowledged.

‡ Fellow of the Alfred P. Sloan Foundation.

[1] Abbreviations: NMR, nuclear magnetic resonance; EDTA, ethylenediaminetetraacetic acid; oligo(U), oligo(uridylic acid); poly(A), poly(adenylic acid); tRNA, transfer ribonucleic acid; EtBr, ethidium bromide; Et, ethidium ion; DH, double helix; T_m, melting temperature.

0006-2960/83/0422-3336$01.50/0

WP-80 FT spectrometer at 32.4 MHz or a superconducting Nicolet NTC-200 spectrometer at 80.9 MHz (^{31}P). For the high-field NMR studies, the nucleic acid solution plus 20% D_2O for field locking was placed in a Wilmad spherical microcell which in turn was inserted into a 20-mm outer diameter NMR tube containing distilled water. In the low-field NMR studies, the sample was placed in a 5-mm NMR tube. Sample volume for low-field spectra was 0.4–0.5 mL; for high-field spectra, it was 2 mL.

High-field, Fourier-transform ^{31}P NMR spectra were taken on the Nicolet 200 spectrometer by using 56° pulses, 4–16K data points, and a 1.4-s recycle time. At low field, 67–75° pulses, 4–8K data points, and 2.0-s recycle times were used. The spectra were broad-band ^1H decoupled. The temperature of the sample was controlled to within ±1 °C by Bruker or Nicolet (on the NTC-200 spectrometer) temperature control units using nitrogen gas as a coolant. Decoupling at the superconducting field produced about 2–6 °C heating of the sample above the gas stream measured temperatures, even when a gated two-level decoupling procedure was used [see Gorenstein & Luxon (1979)]. The ^{31}P "thermometer" described previously was used (Gorenstein et al., 1981) in order to correct for the solution heating by the decoupler.

All chemical shifts were referenced to 85% phosphoric acid in D_2O (0.00 ppm) at room temperature (25 °C). This sample is 0.453 ppm downfield from 15% H_3PO_4 with an external D_2O lock which was used in some earlier publications. Positive chemical shifts are downfield from phosphoric acid.

tRNA spectral changes were reversible except that prolonged heating of some samples at higher temperatures sometimes produced <1% nicks in the phosphodiester backbone. This was shown by the appearance of 2′,3′-cyclic nucleotide ^{31}P signals (Gueron & Shulman, 1975; Gorenstein & Kar, 1975) at ~20 ppm and additional phosphate monoester signals (3–4 ppm). All $tRNA^{Phe}$ originally had no nicks in the backbone. T_1 measurements were performed as described previously (Gorenstein & Luxon, 1979).

UV Spectra, Melting Curves, and Mixing Plots. UV spectra were taken on a Varian/Cary 210 UV–vis spectrophotometer equipped with the capability for direct plotting of absorbance vs. temperature. Melting curves were obtained by monitoring spectral changes at 260 nm with slow cooling (<0.5 °C/min) of the sample through the melting transition (80–4 °C).

Melting temperatures, T_m, represent the midpoint of the transition unless otherwise specified and are little different (±2 °C) from the T_m's defined by the inflection point in the curves. Little hysteresis (±2 °C) in the T_m was observed if the same samples were slowly heated through the transition.

Preparation of Et Ion. Ethidium bromide was purchased from Sigma. For removal of any metal ion impurities, the EtBr was passed through a column of Chelex-100 ion-exchange resin. The Et was strongly absorbed on the resin and was eluted with increasingly concentrated aqueous ammonium bicarbonate. The eluent was collected and dissolved in double-distilled H_2O and lyophilized. This latter process was repeated 4 times. The purified ethidium ion thus obtained was stored at −5 °C until needed.

The Et was dissolved in the appropriate buffer as needed. The concentration was measured by UV spectroscopy with ϵ_{510} = 4110 (Jones et al., 1978). Thin-layer chromatography on silica gel of some of these solutions using a solvent mixture of 1-butanol–acetic acid–H_2O (1:1.5:1) showed only one component to be present.

In the ^{31}P NMR experiments, Et was dissolved in the appropriate buffer, and samples were prepared by adding 5–10 μL of 0.03–0.055 M Et solution to the nucleic acid solutions. The concentration of poly(A)·oligo(U) was 35 mM for the low-field spectra and 3.25 mM oligo(U) and 4.29 mM poly(A) for the high-field spectra. The concentration of tRNA was 0.25–0.3 mM. The pH of the nucleic acid solutions was checked after each addition of Et and was readjusted to 7.0 if necessary. In order to avoid hydrolysis of the tRNA samples, it is important to readjust the pH of the tRNA solutions with very slow addition of 0.1 M NaOH at 4 °C with rapid stirring.

In the experiments with an external standard, a 0.046 mM solution of trimethyl phosphate in distilled water is replaced in the 20-mm NMR tube containing the microcell to yield 17.65:76 phosphate:tRNA phosphate. In this experiment, the concentration of tRNA is 0.346 mM.

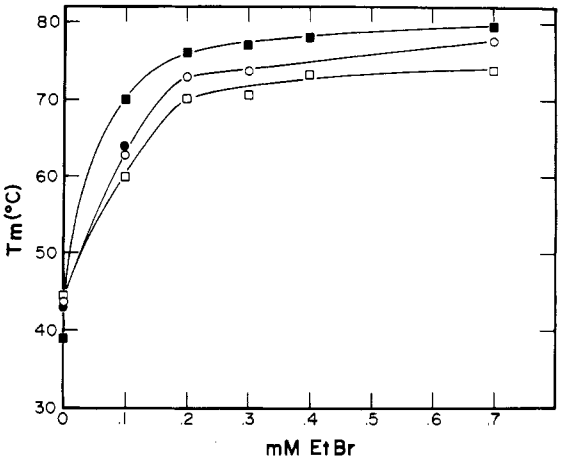

FIGURE 1: Melting temperature of 2:1 (○), 1:1 (□), 1:2 (●), and 1:3 (■) mixtures of poly(A) and oligo(U) as a function of EtBr concentration as measured by UV spectroscopy. Nucleic acid concentration is 2.08 mM in nucleotides in 0.2 M NaCl, 10 mM cacodylate, and 1 mM EDTA, pH 7.

Results

Poly(A)·Oligo(U) Spectroscopy. Melting curves are obtained by monitoring the absorbance changes with temperature of various ratios of poly(A) to oligo(U) and EtBr. A plot of the melting temperature, T_m, as a function of EtBr concentration for various ratios of poly(A) to oligo(U) is ~0.3–0.4 in Figure 1. The T_m values of all the systems are raised as the concentration of EtBr is increased until they level off at ~0.3–0.4 mM EtBr. The concentration of the nucleic acid solutions is 2.08 mM in total nucleotides. In the case of the 1:1 solution, it is 1.04 mM in potential base pairs. Thus, the saturating levels are at an EtBr to nucleotide ratio of 17%. The T_m values increase 26 °C for the 1:1 ratio, 34 °C for the 1:2 ratio, and 40 °C for the 1:3 ratio.

The T_m's vs. EtBr concentration for a 1:1 sample of poly(A)·oligo(U) in 10 mM Mg^{2+} are shown in Figure 2. Here, the rise in T_m is 11–16 °C, depending on whether inflection points or midpoints are used. (This experiment gave a larger discrepancy between the two methods than any other.) The exact T_m's depend a good deal on the length of the oligo(U). Previous work with a different lot of oligo(U) gave melting temperatures ~10 °C lower than present ones in the 0 Mg^{2+} concentration study, but the overall trends were identical (V. Bowie, unpublished results).

^{31}P NMR spectra of poly(A)·oligo(U) at a 1:1 ratio are shown in Figure 3. At high temperature, the spectra correspond to the superposition of the individual nucleic acid components. The downfield signal at −0.053 ppm (60 °C) is the oligo(U). The upfield signal corresponds to poly(A). The smaller peaks are due to heterogeneity of the samples as

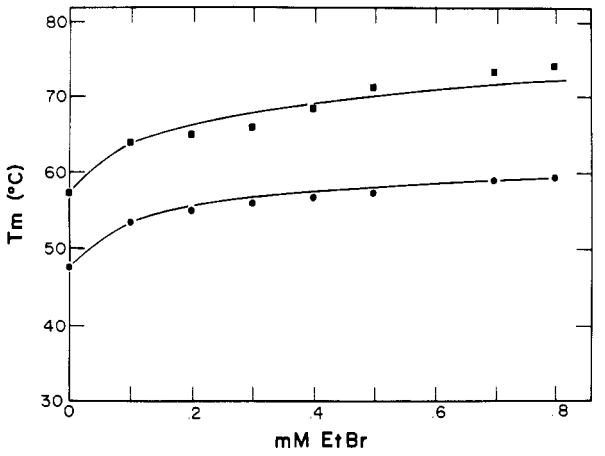

FIGURE 2: Melting temperature of a 1:1 mixture of poly(A)·oligo(U) in 10 mM Mg^{2+} as a function of EtBr concentration. Other conditions same as those in Figure 1. (■) T_m measured from inflection point; (●) T_m measured from midpoints.

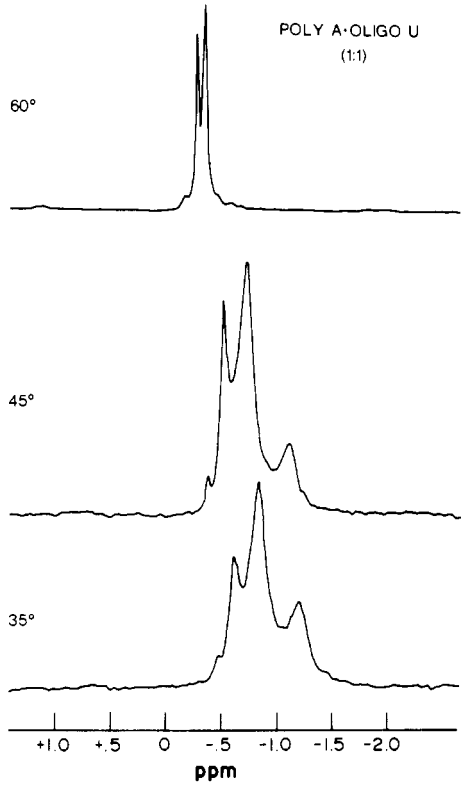

FIGURE 3: ^{31}P NMR spectra for poly(A)·oligo(U) (1:1) at various temperatures in 0.2 M NaCl, 10 mM cacodylate, 1 mM EDTA, pH 7.0, and 20% D_2O at 32.4 MHz. Total nucleotide concentration is 24 mg/mL. Exponential line broadening is 1 Hz.

discussed in Gorenstein et al. (1982). At temperatures below the T_m of 48 °C, a new broad signal appears 0.4–0.6 ppm upfield from the single-strand nucleic acids. We have assigned this upfield signal to the resonance of phosphates in double–triple helices (Gorenstein et al., 1982).

In Figure 4, we show the ^{31}P spectra of a (1:1:3) sample of poly(A):oligo(U):Et. A new broad signal at ~0.55 ppm appears approximately 2 ppm downfield from the multistrand helix signal at −1.45 ppm. This signal arises from phosphates which are perturbed due to intercalated ethidium (see Discussion). The ^{31}P melting curve for the signals in Figure 4 is also shown in Figure 5. The melting temperature as given by these data is ~62 °C, considerably higher than the melting temperature of the double helix in the absence of Et (Gorenstein et al., 1982).

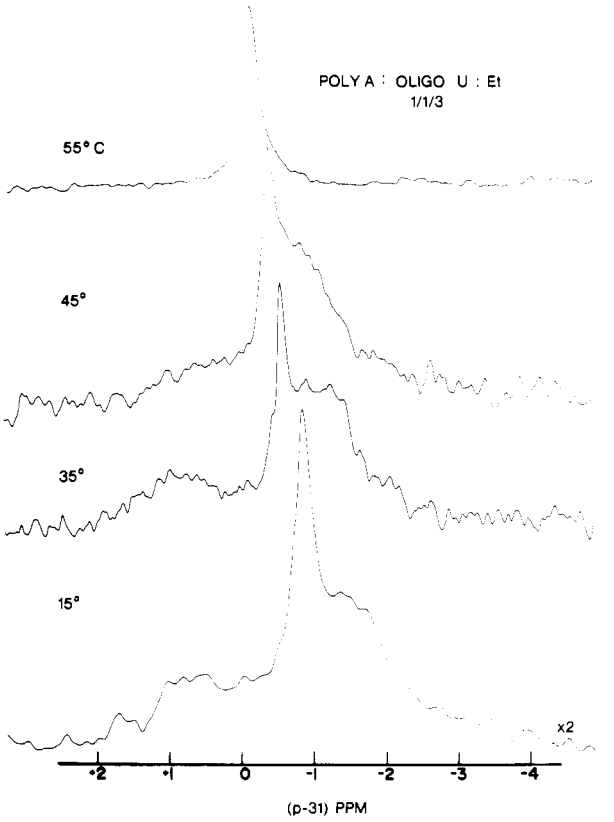

FIGURE 4: ^{31}P NMR spectra of poly(A)·oligo(U)·Et (1:1:3) at various temperatures under the same conditions as those in Figure 3.

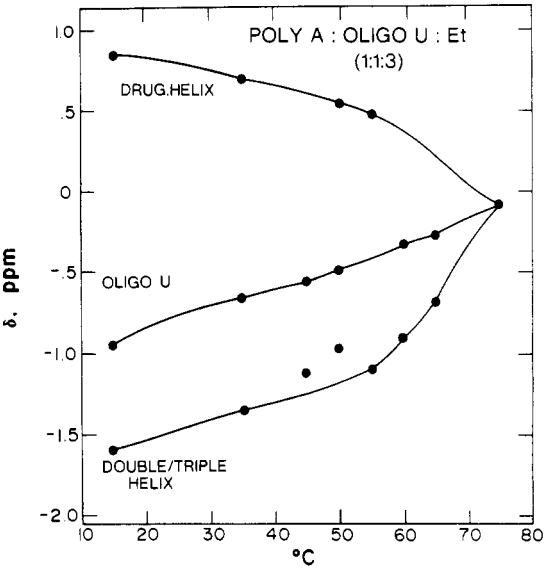

FIGURE 5: ^{31}P melting curves for signals in Figure 4.

^{31}P NMR of Poly(A)·Oligo(U) in 10 mM $MgCl_2$. ^{31}P spectra of poly(A)·oligo(U) with and without added Et are shown in Figure 6. In the absence of Et in Mg^{2+} buffer, at 31 °C we have two peaks; the downfield peak is due to oligo(U), and the upfield peak is due to poly(A) superimposed on the double-helix phosphates. In the presence of 10 mM Mg^{2+}, the oligo(U) and poly(A) resonances are shifted 0.3–0.5 ppm upfield so that the poly(A) peak obscures the double-helix peaks. The longitudinal relaxation times, T_1, measured for a 1:1 sample of poly(A)·oligo(U) at 40 °C are 1.97 ± 0.11 s for oligo(U), 1.005 ± 0.069 s for the double helix, and 1.69 ± 0.081 s for poly(A). The T_1 for poly(A) is less certain than the others since the double helix is superimposed, but the number agrees roughly with other measurements on poly(A)

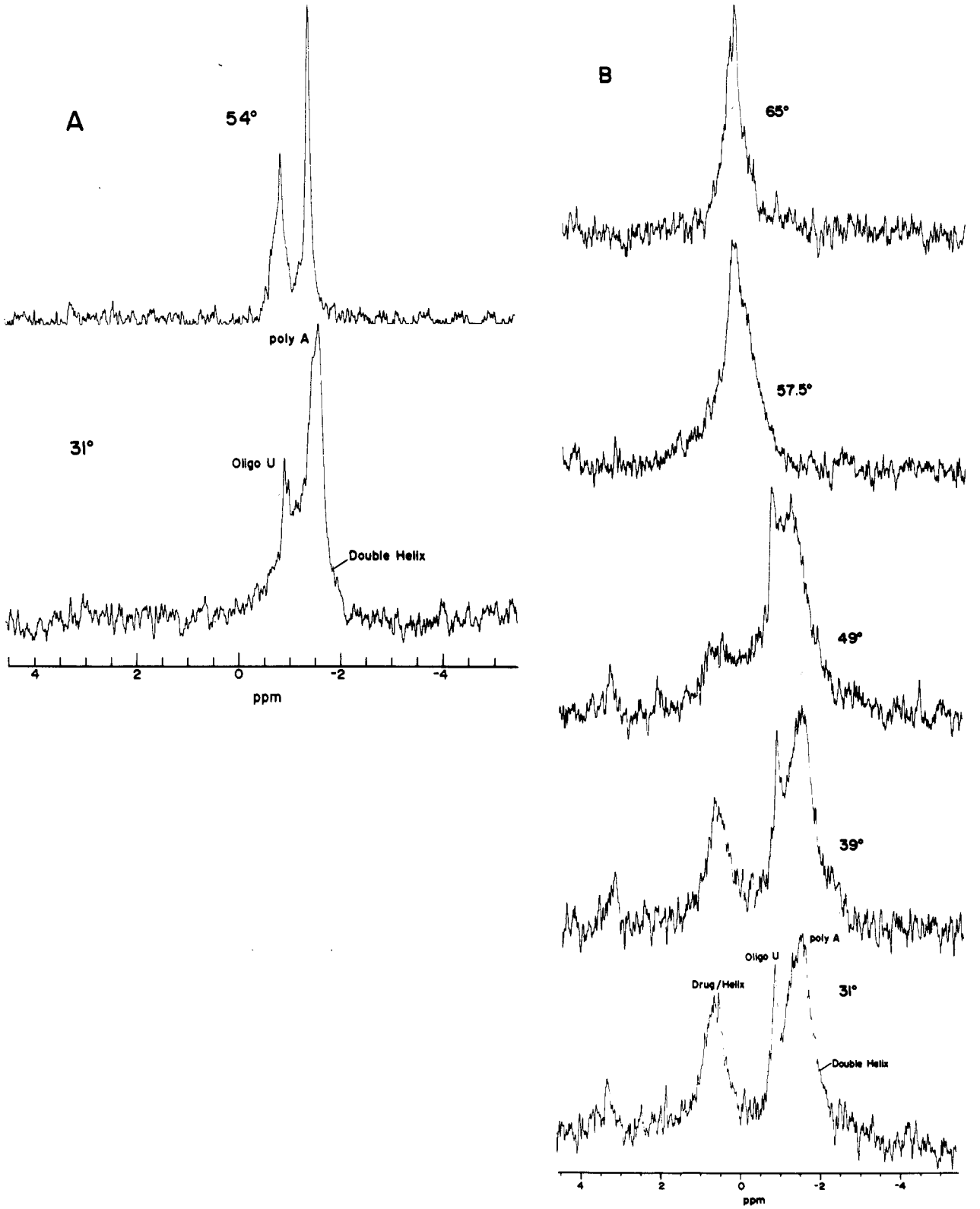

FIGURE 6: (A) ^{31}P NMR spectra of poly(A)·oligo(U) (1.32:1) in 10 mM $MgCl_2$ at 80.99 MHz. Total nucleotide concentration is 8.4 mM. Exponential line broadening is 2 Hz. Other conditions same as those in Figure 4. (B) ^{31}P NMR spectra of poly(A)·oligo(U)·Et (1.32:1.00:0.62) at various temperatures. Conditions same as those in part A.

alone (Akasaka, 1974). On the basis of the above relaxation times, the poly(A):oligo(U) ratio of 1.32, and the relative integrals of the two peaks, we can calculate that 27–32% of the phosphates are in double-helix resonances at 31 °C in the absence of EtBr.

In the presence of Et and Mg^{2+}, we again have a downfield peak at 0.55 ppm. As the temperature is raised, the downfield peak first broadens and suddenly shifts upfield to merge with the upfield double-helix peak at 57.5 °C. When heated further, the broad resonance narrows, but the double helix is still visible at 65 °C (compare to 54.0 °C spectra in the absence of Et). In Figure 7, we show a melting curve for these resonances which indicates a melting temperature of 57–58 °C.

The percent of total phosphate signal represented by the downfield signal can be estimated from the ratio of the downfield peak integral to the total integrated intensity. Two

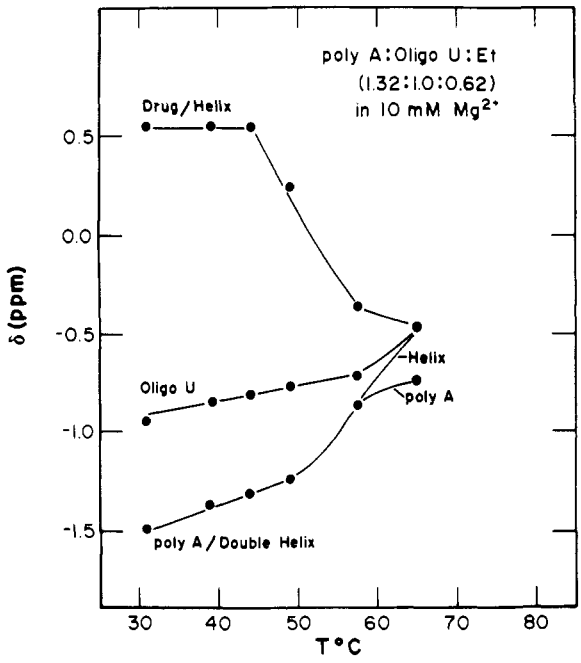

FIGURE 7: ^{31}P melting curves for signals in Figure 6B.

Table I: Percent of Total Phosphates Represented by Drug-Helix Peak

temp (°C)	% drug-helix[a]	% drug-helix[b]
31	30	34
39	25	29
44	24	27
49	21	24

[a] Based on T_1 of drug-helix peak = 1.00 and T_1 of remaining peaks = 1.97. [b] Based on T_1(drug-helix) = T_1(remaining peaks).

limiting cases were considered. The first assumes that the T_1 of the downfield signal is 1.0 s and that all the upfield resonances relax at the oligo(U) relaxation time, T_1 = 1.96 s. The second assumes that all the signals relax at the same rate. As can be seen in Table I, the difference between the two assumptions is 3–4%, which is within the experimental error. Differential NOE effects between the various signals will also produce only modest changes in the integrated intensities (Gorenstein et al., 1982). The percent of total phosphate signal intensity represented by the downfield peak is given in Table I.

tRNA ^{31}P Spectra. The ^{31}P spectra of tRNA plus ethidium at 31 °C are shown in Figure 8. The chemical shifts of the scattered peaks are virtually unaffected with one possible exception. However, a number of peaks undergo significant line broadening as a function of added ethidium (Figure 9). The only peak in the downfield portion of the spectrum (+3.3 to −0.453 ppm) which broadens is peak E at ~0.245 ppm. The line width of this peak goes from ~15 Hz at 0.0 Et:tRNA to >25 Hz when the Et:tRNA ratio is increased to 1.32. At an Et:tRNA ratio of 2.0, the peak cannot be detected as a separate peak. It is possible that the chemical shift of peak E moves upfield to coincide with peak F at ~0.077 ppm. However, the intensity of peak F with added Et increases only slightly. This can be explained by the superposition of a broadened peak E under the sharper peak F. The entire upfield portion of the spectrum (−1.85 to −4.53 ppm) broadens and loses resolution as the Et:tRNA ratio increases. Peaks N, O, P, and Q between −1.853 and −2.653 ppm broaden and merge into one another. Peaks R/S and T also broaden as

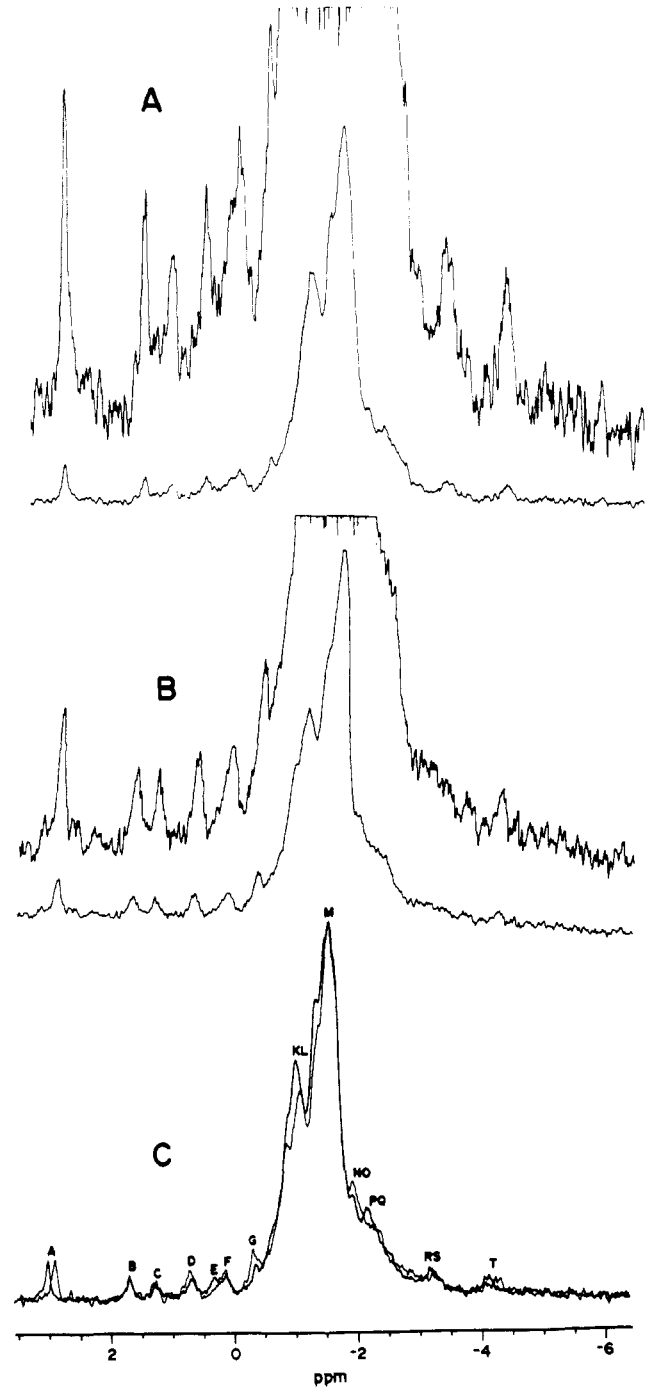

FIGURE 8: ^{31}P NMR spectra of $tRNA^{Phe}$ at various molar ratios of Et in 10 mM $MgCl_2$, 0.1 M NaCl, 10 mM cacodylate, 1 mM EDTA, pH 7.0, and 20% D_2O, 31 °C and 80.99 MHz. Exponential line broadening is 2Hz. Et/tRNA ratio of (A) 0.44, (B) 1.32, and (C) 2.0; thin curve, with drug; thick curve, without drug.

a function of added Et (Figure 9). These upfield peaks and peak E narrow as the temperature is raised up to 49 °C. Between 49 and 55 °C, peaks R/S and T again begin to broaden as the temperature is increased. Peak U (Gorenstein & Luxon, 1979) is not visible in these spectra.

The other downfield peaks show no significant line broadening or changes in intensity within experimental error. Peak A especially remains narrow, which contrasts with its linewidth behavior due to added Mn^{2+} (Gorenstein et al., 1981), where A shows a rapid linear increase in line width at low Mn^{2+}:tRNA ratios. This result gives us confidence that the line-broadening effects are not due to paramagnetic metal ion impurities in the Et solution.

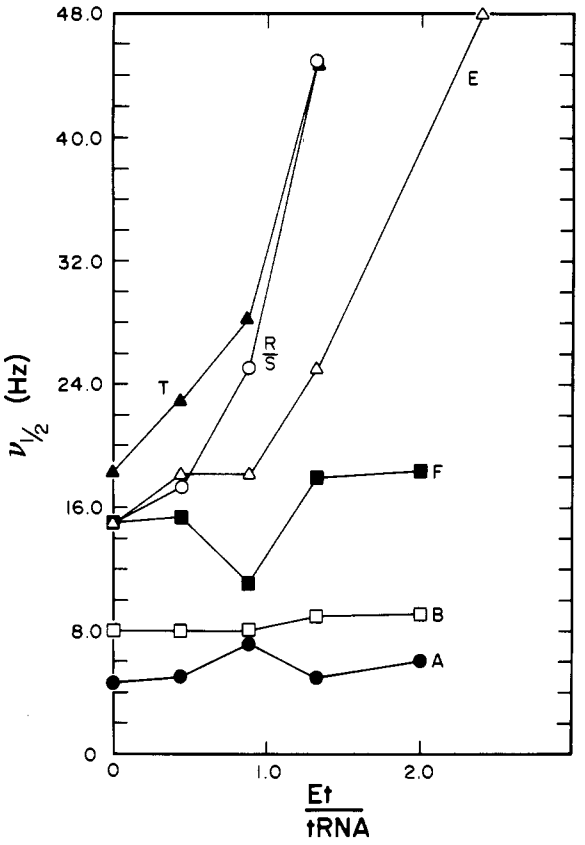

FIGURE 9: Plot of the corrected line widths at half-height at 80.99 MHz vs. the molar ratio of Et for selected signals from Figure 8: peak A (●), peak B (□), peak F (■), peak E (△), peak R/S (○), and peak T (▲).

At an Et:tRNA ratio of 1.32 and above, there possibly is a small new peak at 0.847 ppm which appears as a shoulder to peak D (0.7 ppm). This peak is a consistent feature of three out of four 31 °C spectra at the higher Et ratios and of the 35 and 39 °C spectra as well.

The results of the experiments with an external phosphate standard at 31 and 44 °C revealed that the percentage of external phosphate to total phosphate increases by only 1.63% as the Et ratio goes from 0 to 1.75. Since the experimental uncertainty in the integrals is at least 3%, we cannot determine if a small amount of overall intensity is lost. However, at most, this represents a loss of seven phosphates, so there is no large-scale loss of intensity as Et binds.

Discussion

^{31}P Chemical Shifts and Et Binding to Nucleic Acids. Gorenstein & Kar (1975) have attempted to calculate the ^{31}P chemical shifts for a model phosphate diester in various geometries. These calculations revealed that ^{31}P chemical shifts should be dependent on P–O ester torsional angles (ω,ω') and O–P–O bond angles. These shift calculations suggested that a phosphate diester in a gauche,gauche (g,g)[2] conformation should have a ^{31}P chemical shift substantially upfield (by at least several ppm) from a phosphate diester in a gauche,trans (g,t) conformation [see also Prado et al. (1979)].

These insights into ^{31}P chemical shifts apply directly to the ^{31}P spectra of nucleic acid–drug complexes. In one of the earliest clear demonstrations of ^{31}P spectra perturbations upon drug binding, Patel (1976) and Reinhardt & Krugh (1977) showed that actinomycin D (Act D) shifted several phosphate diester signals up to 2.6 ppm downfield from the double-helical signal upon binding to oligonucleotide duplexes containing dGdC base pairs. Thus, downfield ^{31}P shifts of 1.6 and 2.6 ppm in the dCdGdCdG·Act D (2:1) complex and 1.6 ppm in the pdGdC·Act D (2:1) complex at 8 °C have been observed. Reinhardt & Krugh (1977) showed that at even lower temperature (−18 °C) in methanol–water the ^{31}P signals of the two phosphates in duplex pdGdC are split into two signals and shifted 1.7 and 2.4 ppm downfield upon complexation with Act D. These shifts are consistent with the Jain & Sobell (1972) model for these intercalated complexes: partial unwinding of a specific section of the double helix allows these planar, heterocyclic drugs such as Act D to stack between two base pairs. Recent X-ray studies on various intercalating drug duplex complexes (Reddy et al., 1979; Shieh et al., 1980) suggest that the major backbone deformation of the nucleic acid upon intercalation of the drug involves the C5′–O5′ torsional angle. However, in several complexes [see Reddy et al. (1979)], the ω,ω' torsional angles are altered from the normal values of 290°,290°, ($-g,-g$) to values such as 273°,323°. According to the calculations on ^{31}P chemical shifts, such torsional angle perturbations of 20–30° can result in ^{31}P deshielding of ca. 0.5–1.0 ppm. Either the actual solution ω,ω' torsional angle changes for these drug complexes are somewhat larger than indicated by the X-ray studies or some other effect, such as bond angle distortion or the C5′–O5′ torsional angle changes, also contributes to the larger observed shift perturbations.

The downfield shifts which we observed in the poly(A)·oligo(U)·Et complex are similar to the Act D effects. This deshielding for the drug complex signal is entirely consistent with the intercalation perturbation of the phosphate ester geometry observed in the Act D complexes. The unperturbed helix signals at 1.453 ppm in these complexes likely represent undisturbed phosphates in regions adjacent to the intercalation site. Hogan & Jardetzky (1980) in an NMR study of EtBr binding to DNA found that the effects of the intercalation are localized to a two base pair long DNA region and that internal motions outside the binding site are nearly unaffected.

Surprisingly, however, other EtBr complexes of nucleic acids show smaller ^{31}P shift changes (Patel & Canuel, 1977; Reinhardt & Krugh, 1977). In fact, except for the results shown in Figures 4–7 and the studies of Patel and Krugh on Act D, all other drug–duplex complexes show only small changes in the ^{31}P NMR spectra (Patel & Canuel, 1977; Reinhardt & Krugh, 1977; Wilson & Jones, 1982). Thus, Reinhardt & Krugh (1977) have shown that the drugs EtBr and 9-aminoacridine produce small (0.2 ppm) upfield and downfield shifts upon complexation with complementary and noncomplementary deoxydinucleotides at 3–6 °C.

It is significant that the large Et-induced ^{31}P shift shown in Figures 4–7 is *not* observed in low salt poly(A)·oligo(U) solution (Gorenstein, 1978). It is possible that in these low salt solutions the main interactions between the drug and the nucleic acids are electrostatic. Consistent with this interpretation, the purely electrostatic association between the antibiotic netropsin and the self-complementary duplex dGdGdAdAdTdTdCdC produces only small upfield ^{31}P shifts (Patel, 1979a–d). This (and other data) supports a drug–complex model involving binding at dAdT base pairs in the minor groove with the two charged guanidine ends of the drug electrostatically associating with the phosphates. These small

[2] We should mention at this time that for purposes of conveniently describing the torsional dependence of chemical shifts, we generally make no distinction between ROPO(R) torsional angles (ω) +60° (+g) or −60° (−g). In addition ω,ω' torsional angles of g,t, $-g,t$, t,g, and $t,-g$ will often be simply grouped together as g,t. similarly, g,g includes conformers $-g,-g$, $g,-g$, and $-g,g$, although the latter two conformers do have different ^{31}P chemical shifts from g,g.

upfield shifts are similar to the nonspecific Mg^{2+} ion effects on the duplex signals in tRNA (Gorenstein et al., 1981; Gueron & Shulman, 1975). This further supports the hypothesis that large (2 ppm) downfield shifts are only observed for the intercalation mode of drug binding.

Wilson & Jones (1982) have measured the ^{31}P chemical shift change induced in DNA by various drugs: ethidium, quinacrine, daunorubicin, and tetralysine. They find a linear correlation between the change in chemical shift and the unwinding angle of the DNA double helix measured for each drug.

Stabilization of the Double Helix by Et. Both UV and ^{31}P NMR spectroscopies demonstrate the stabilization of the double helix by Et. The rise in T_m with increased concentration of Et as shown in Figures 1 and 2 illustrates this effect. In the 31 °C ^{31}P NMR spectra in the presence of 10 mM Mg^{2+}, we estimate that the downfield drug–helix peak accounts for ~30% of the integrated intensity. According to the nearest-neighbor exclusion hypothesis, Et binds to every other base pair under saturating conditions (Bresloff & Crothers, 1975). If 50% of the double-helix phosphates are represented by this peak, then 60% of the phosphates are in double-helix conformations in this 1.32:1.0 poly(A):oligo(U) system. In the absence of Et under the same conditions, we estimate that ~31% of the potential base pairs are in double-helix conformations.

The systems in which the poly(A):oligo(U) ratio differs from 1:1 have a lower T_m (Figure 1) in the absence of Et, presumably because the number of potential base pairs is fewer (the total number of nucleotides was held constant) and helix formation is less favored. However, the systems with oligo(U):poly(A) > 1 have not only a higher rise in T_m but also a higher absolute T_m with saturating Et. This is not true for an oligo(U):poly(A) ratio of 0.5 (V. Bowie, unpublished results). It is not certain what causes this effect, but perhaps the Et also stabilizes the triple helix which is formed at higher oligo(U):poly(A) ratios.

Both the ^{31}P and UV results in 10 mM Mg^{2+} show that the effects of Et are no greater and perhaps less pronounced than in its absence. Waring (1965) notes that the binding of Et to DNA and RNA is reduced in the presence of Mg^{2+} and attributes this to an increase in the dissociation rate constant and not to a decrease in binding sites. In tRNA, Mg^{2+} (as well as spermine and spermidine) competes for ethidium binding sites (Sakai et al., 1975). It is likely that in the non-Mg^{2+} solutions, both the electrostatic and intercalation effects of Et are used to stabilize the double helix.

The melting of Et complexes as monitored by ^{31}P NMR spectroscopy shows the result of chemical exchange broadening. The narrower peaks in the 10 mM Mg^{2+} samples at low temperature are probably mainly due to the higher spectrometer frequency since the slow exchange region which give rise to narrow separate peaks is determined by $\tau/(2\pi\Delta\nu) \gg 1$, where τ is the lifetime of a given state. At 32 MHz, $\Delta\nu$ will be 2.5 times smaller than at 81 MHz so that the slow exchange region will occur at lower temperatures at lower spectrometer frequency. Figure 6 illustrates nicely the effects of chemical exchange. The line widths remain narrow, and there is little change in the separation of the signals until ~49 °C when the upfield peak broadens dramatically. At 57 °C, the peaks merge and begin to narrow. The region of maximal line broadening occurs at intermediate exchange between these two temperatures. In this region, we can estimate the lifetime of the state from the formula $\tau = 2^{1/2}/(2\pi\Delta\nu)$ as between 1 and 3 ms.

In their ^{31}P NMR work on EtBr·DNA complexes, Wilson et al. (1981) and Wilson & Jones (1982) observe downfield shifts and line broadening as a function of the EtBr:DNA ratio, but they do not observe a separate drug–helix signal. Under their conditions and magnetic field strength, they are in fast chemical exchange on the basis of temperature-jump kinetic studies (Bresloff & Crothers, 1975; Wakelin & Waring, 1980). However, the relaxation times of an EtBr·poly(A)·poly(U) system are from 5 to 10 times larger than those for calf thymus DNA (Bresloff & Crothers, 1975). At 81 MHz and low temperature, our poly(A)·oligo(U)·Et system is clearly in slow chemical exchange.

Effects of Et on tRNA. Fluorescence depolarization studies indicate that in the presence of Mg^{2+} there is one strong binding site for Et to $tRNA^{Phe}$ (Tao et al., 1970; Wells & Cantor, 1977) and perhaps a weaker site (Sturgill, 1978). The binding constant for the stronger site is $(4–5) \times 10^5$ M^{-1} and for the weaker site is $\sim 4 \times 10^4$ M^{-1} at temperatures of 22–25 °C (Sakai & Cohen, 1976; Sturgill, 1978; Torgerson et al., 1980). Lifetime measurement studies indicate that at low Et:tRNA ratios, the fluorescence decays with a single lifetime of 28 ms and at higher ratios the decay contains shorter lived components as well (Jones et al., 1978). Wells & Cantor (1977) have determined that the binding site of Et to tRNA is between 33 and 40 Å from the 3′ end of the tRNA. However, Tao et al. (1970) have shown that in the presence of Mg^{2+} the binding of Et is very far away from the Y base (anticodon loop) while in the absence of Mg^{2+} it binds closely to the Y base.

On the basis of relaxation studies (Tritton & Mohr, 1971), fluorescence lifetime and steady-state fluorescence studies (Jones et al., 1978), and especially NMR studies (Jones & Kearns, 1975; Jones et al., 1978), the major mode of binding of EtBr to $tRNA^{Phe}$ is believed to be intercalation between base pairs AU6 and AU7 (or AU5-AU6) of the acceptor stem. The interpretation has received wide acceptance among many authors. However, the X-ray diffraction studies of crystals of tRNA into which EtBr has been allowed to diffuse indicate another mode of binding. The ethidium is found to lodge in a cavity at the mouth of the P10 loop of the tRNA tertiary structure, stacked over U8 which is involved in the tertiary base pair U8-A14 (Liebman et al., 1977) (Figure 10). Liebman et al. (1977) have reinterpreted the fluorescence and NMR data in light of this mode of bonding.

Our results do not resolve the controversy but do lend some support to the view that the Et lodges itself in the tertiary pocket. The $tRNA^{Phe}$ ^{31}P spectra consist of a major cluster at −0.433 to −1.453 ppm with both upfield and downfield scattered signals. It has been suggested that bond and torsional angle differences account for the 7 ppm spread in the ^{31}P signals of tRNA (Gorenstein & Luxon, 1979). These scattered signals arise from phosphates which differ in conformation from the $-g,-g$ conformation and geometry of normal RNA double helices and are attributed to phosphates associated with the tertiary interactions and with certain phosphates in the AC loop (Gueron & Shulman, 1975; Salemink et al., 1979; 1981; Gorenstein & Luxon, 1979; Gorenstein et al., 1981; Gorenstein & Goldfield, 1982a,b).

Based upon the poly(A)·oligo(U) results, one would except that the major result of intercalation in the ^{31}P NMR spectra would be a downfield shift of one or two phosphates from the central cluster region to 0.5–0.8 ppm. It is possible that the small peak at 0.847 ppm is due to phosphates at the intercalation site. However, we do not see any major (one to two phosphates) growth in intensity in this spectral region.

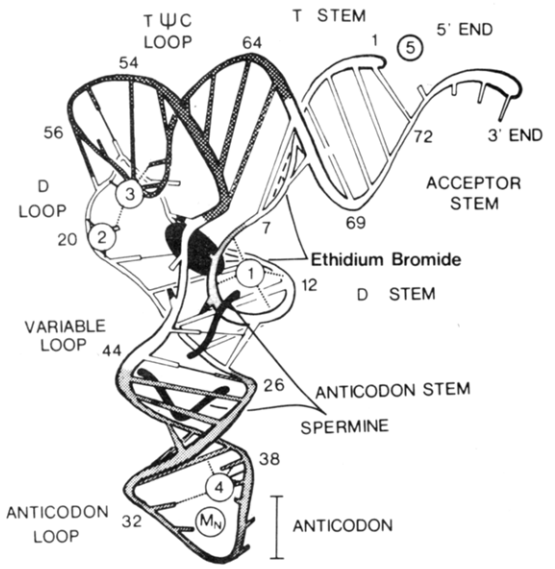

FIGURE 10: Schematic model for three-dimensional structure of yeast $tRNA^{Phe}$ showing sugar–phosphate backbone, base pairs, five magnesium binding sites (numbered circles), magnesium site, and proposed ethidium bromide and spermine binding sites. Partially derived from Holbrook et al. (1977), Kim (1979), and Liebman et al. (1977).

The most striking effect of the addition of Et is the major broadening of the upfield scattered peaks which have been associated with tertiary interactions of the TψC and D stems and of peak E. On the basis of its temperature and Mg^{2+} and Mn^{2+} dependence, we have previously suggested that this peak is associated with the AC loop (Gorenstein et al., 1981; Gorenstein & Goldfield, 1982a,b). However, peak E, like the broadened peaks in the upfield spectral region, must be associated with tertiary interactions near the Et binding site. Since the Et binding is neither near nor in the AC loop, we may conclude that peak E is likely not in this loop. Peak E broadens at low Mn^{2+}:tRNA ratios so that it is very likely associated with one of the paramagnetic metal ion binding sites. Proton NMR studies on yeast $tRNA^{Phe}$ by Hurd et al. (1979) have indicated that the first manganese(II) binding site is the phosphate of U8 and A9 in the loop between the acceptor and D stems (see Figure 10). Of all the proposed paramagnetic sites [see Gorenstein et al. (1981) and references cited therein], this is closest to either of the proposed Et binding sites and could possibly be associated with peak E. It is significant that peak E also broadens upon the addition of spermine to tRNA (Gorenstein & Goldfield, 1982b). One of the bound spermine molecules which has been resolved in the X-ray structure of $tRNA^{Phe}$ (Quigley et al., 1978) binds so that it is more or less wrapped around phosphate 10 at the beginning of the D system. The upper NH_3^+ group is close to phosphate 9, although not in hydrogen-bonding contact (Figure 10).

Our interpretation of the broadening of the various ^{31}P resonances is that the resonances of phosphates near the Et binding sites are affected because the phosphates are held more rigidly when Et is bound. Thus, if the Et rests in the tertiary pocket described above, or if it intercalates in the acceptor stem, it is likely that the phosphate motions near where the acceptor stem joins the D stem will be slowed down, while the overall tumbling of the molecule will be affected only slightly. Therefore, the line widths of the terminal phosphate, those in the AC loop, and others will remain narrow. Bolton & James (1979) and others have shown that to account for the ^{31}P relaxation behavior of nucleic acids at least two correlation times are required, a slow time (milliseconds) associated with long-range bending (or tumbling) and a faster (0.3–0.5 ns) time associated with rotational wobbling about P–O ester bonds. If the Et restricts the local flexibility of phosphates involved in tertiary interactions near the binding site, then the differential broadening of the scattered peaks could be explained.

The effect of temperature on the ^{31}P NMR spectra of the tRNA·Et complex is consistent with the ^1H NMR work of Jones & Kearns (1975), who also see a lessening of Et binding effects above 30 °C. Thus, the narrowing of the broadened peaks as the temperature is raised is probably due mostly to a decrease in Et binding at higher temperatures.

In our previous work (Gorenstein & Luxon, 1979; Gorenstein et al., 1981; Gorenstein & Goldfield, 1982a,b), we have presented evidence to support the existence of at least two different tertiary structures in a number of different tRNAs. We have also characterized the conformations in terms of a high-temperature–low Mg^{2+} concentration conformation and a low-temperature–high Mg^{2+} concentration conformation which is presumably that found in the crystal structure. We will briefly summarize this evidence on the basis of previous ^{31}P work.

For most of the tRNA species, peaks C, D, E, F, P, T, and U shift with temperature between 22 and 60 °C. The line widths for the resolvable peaks, especially T and U, are similarly temperature sensitive. The line widths of peaks U and T show evidence of chemical exchange broadening and narrowing as a function of temperature. Peaks A, C, E, F, P, and T/U are also sensitive to Mg^{2+} concentration. Peak E moves away from the central peak region (downfield) both when temperature is increased and when Mg^{2+} concentration is decreased at 19 °C. Peak T is relatively constant with temperature, but it resonates 0.3 ppm downfield at zero Mg^{2+} concentration from its resonance at 10 mM Mg^{2+}.

We have characterized the low-temperature transition as an interconversion of two conformations of the AC loop (Gorenstein & Goldfield, 1982a,b) and have assigned peak C to the phosphate of Y37 and either E or U to the phosphate of U33 (Gorenstein et al., 1981). Since peak E appears now not to be in AC loop, we can assign peak U to this phosphate. It is interesting to note that in *Escherichia coli* $tRNA^{fMet}$ peak U is far less temperature dependent than in other tRNAs (Gorenstein & Goldfield, 1982a,b). It is also true that in $tRNA^{fMet}$ the conformation of U33 differs from that in $tRNA^{Phe}$, according to the crystal structure [see Gorenstein & Goldfield (1982b) and references cited therein]. It is also likely that peak F is in the AC loop (Salemink et al., 1979, 1981).

The temperature and Mg^{2+} concentration dependences of peaks E and T, which, on the basis of this study, are not in the AC loop, give evidence that the change in anticodon loop structure which we have put forward is accompanied by further changes in tertiary structure as either the temperature is raised or the Mg^{2+} ion concentration is decreased. It is interesting that peak E moves downfield, since such a shift represents a shift away from a *g,g* conformation to a *g,t* conformation. This downfield shift with temperature is observed in other tRNAs as well and could represent a conformational change common to many tRNA molecules.

Acknowledgments

We acknowledge the contributions of Donna Vegeais and Rouhlwai Chen to these studies.

References

Akasaka, K. (1974) *Biopolymers 13*, 2273.

Bolton, P. H., & James, T. L. (1979) *J. Phys. Chem. 83*, 3359.
Bresloff, J. L., & Crothers, D. M. (1975) *J. Mol. Biol. 95*, 103.
Gorenstein, D. G. (1975) *J. Am. Chem. Soc. 97*, 898.
Gorenstein, D. G. (1978) *Jerusalem Symp. Quantum Chem. Biochem. 11*, 1–15.
Gorenstein, D. G. (1981) *Annu. Rev. Biophys. Bioeng. 10*, 355.
Gorenstein, D. G. (1983) *^{31}P NMR: Principles and Applications*, Academic Press, New York and London.
Gorenstein, D. G., & Kar, D. (1975) *Biochem. Biophys. Res. Commun. 65*, 1073.
Gorenstein, D. G., & Luxon, B. A. (1979) *Biochemistry 18*, 3796.
Gorenstein, D. G., & Goldfield, E. M. (1982a) *Mol. Cell. Biochem. 46*, 97–120.
Gorenstein, D. G., & Goldfield, E. M. (1982b) *Biochemistry 21*, 5839.
Gorenstein, D. G., Findlay, J. B., Momii, R. K., Luxon, B. A., & Kar, D. (1976) *Biochemistry 15*, 3796.
Gorenstein, D. G., Goldfield, E. M., Chen, R., Kovar, K., & Luxon, B. A. (1981) *Biochemistry 20*, 2141.
Gorenstein, D. G., Luxon, B. A., Goldfield, E. M., Lai, K., & Vegeais, D. (1982) *Biochemistry 21*, 580.
Gueron, M., & Shulman, R. G. (1975) *Proc. Natl. Acad. Sci. U.S.A. 72*, 3482.
Hogan, M. E., & Jardetzky, O. (1980) *Biochemistry 19*, 2079.
Holbrook, S. R., Sussman, J. L., Warrant, R. W., Church, G. M., & Kim, S.-H. (1977) *Nucleic Acids Res. 4*, 2811.
Hurd, R. E., Azhderian, E., & Reid, B. R. (1979) *Biochemistry 18*, 4012.
Jain, J. C., & Sobell, H. M. (1972) *J. Mol. Biol. 68*, 21.
Jones, C. R., & Kearns, D. R. (1975) *Biochemistry 14*, 2660.
Jones, C. R., Bolton, P. H., & Kearns, D. R. (1978) *Biochemistry 17*, 601.
Kim, S.-H. (1979) *Transfer RNA: Structure, Properties, and Recognition* (Schimmel, P. R., Soll, P., & Abelson, J. R., Eds.) p 115, Cold Spring Harbor Laboratories, Cold Spring Harbor, NY.
Kim, S. H., Berman, H. M., Seeman, N. C., & Newton, M. D. (1973) *Acta Crystallogr., Sect. B B29*, 703.
Liebman, M., Rubin, J., & Sundaralingam, M. (1977) *Proc. Natl. Acad. Sci. U.S.A. 74*, 4821.
Patel, D. J. (1976) *Biopolymers 15*, 533.
Patel, D. J. (1979a) *Acc. Chem. Res. 12*, 118.
Patel, D. J. (1979b) in *Stereodynamics of Molecular Systems*, pp 397–472, Pergamon Press, New York.
Patel, D. J. (1979c) *Eur. J. Biochem. 96*, 267.
Patel, D. J. (1979d) *Eur. J. Biochem. 99*, 369.
Patel, D. J., & Canuel, L. L. (1977) *Proc. Natl. Acad. Sci. U.S.A. 73*, 3343.
Prado, F. R., Giessner-Prettre, C., Pullman, B., & Daudey, J.-P. (1979) *J. Am. Chem. Soc. 101*, 1737–1742.
Quigley, G. J., Teeter, M. M., & Rich, A. (1978) *Proc. Natl. Acad. Sci. U.S.A. 75*, 64.
Reddy, B. S., Seshadri, T. P., Sakore, T. D., & Sobell, H. M. (1979) *J. Mol. Biol. 135*, 787.
Reinhardt, C. G., & Krugh, T. R. (1977) *Biochemistry 16*, 2890.
Sakai, T. T., & Cohen, S. S. (1976) *Prog. Nucleic Acid Res. Mol. Biol. 17*, 15.
Sakai, T. T., Torget, R., Freda, C. E., & Cohen, S. S. (1975) *Nucleic Acids Res. 2*, 1005.
Salemink, P. J. M., Swarthof, T., & Hilbers, C. W. (1979) *Biochemistry 18*, 3477.
Salemink, P. J. M., Reijerse, E. J., Mollevanger, L., & Hilbers, C. W. (1981) *Eur. J. Biochem. 115*, 635.
Shieh, H.-S., Berman, H. M., Debrow, M., & Neidle, S. (1980) *Nucleic Acids Res. 8*, 85.
Sturgill, T. W. (1978) *Biopolymers 17*, 1793.
Sundaralingam, M. (1969) *Biopolymers 7*, 821.
Tao, T., Nelson, J. H., & Cantor, C. R. (1970) *Biochemistry 9*, 3514.
Torgerson, P. M., Drickamer, H. G., & Weber, G. (1980) *Biochemistry 19*, 3960.
Tritton, T. R., & Mohr, S. C. (1971) *Biochem. Biophys. Res. Commun. 45*, 1240.
Ts'o, P. O. P. (1975) *Basic Principles in Nucleic Acid Chemistry*, Vol. I and II, Academic Press, New York and London.
Wakelin, L. P. G., & Waring, M. (1980) *J. Mol. Biol. 144*, 183.
Waring, M. J. (1965) *J. Mol. Biol. 13*, 269.
Wells, B. D., & Cantor, C. R. (1977) *Nucleic Acids Res. 4*, 1667.
Wilson, W. D., & Jones, R. L. (1982) *Nucleic Acids Res. 10*, 1399.
Wilson, W. D., Keel, R. A., & Mariam, R. H. (1981) *J. Am. Chem. Soc. 103*, 6267.